Available online at www.sciencedirect.com
SCIENCE DIRECT
Diamond & Related Materials 15 (2006) 875 – 879
DIAMOND AND RELATED MATERIALS
www.elsevier.com/locate/diamond

Electron emission microscopy of nano-crystal graphitic films as high current density electron sources

F.A.M. Koeck [a,*], A.N. Obraztsov [b], R.J. Nemanich [a]

[a] Department of Physics, North Carolina State University, 851 Main Campus Drive, Partners III, Rm 151, Raleigh, NC 27695-8202, USA
[b] Physics Department, Moscow State University, Moscow 119992, Russia

Available online 17 February 2006

Abstract

Electron emission can be described by thermionic and field effects or a combination of both and can be characterized by the laws of Richardson–Dushman and Fowler–Nordheim, respectively. Nano-crystal graphitic films exhibit a film morphology comprised mainly of crystalline graphite sheets which are vertically aligned with respect to the substrate surface. Field emission from these films exhibits a low threshold field of <1 V/μm, an emission site density of ~3×10^5/cm^2 and a significant distribution in brightness. The temperature dependence of the emission is complex and may be influenced by molecular adsorbates and interface reactions. For nano-crystalline graphite films on molybdenum it was found that the emission current is significantly increased with temperature. The results suggest a field dependent barrier which may be an indication of field penetration.

1. Introduction

High brightness electron sources are in strong demand ranging from display and lighting applications to high power microwave tubes. Common to instruments improvement is the employment of efficient electron emitters. Here, nanostructured carbon materials have displayed superior emission characteristics especially high current densities at low threshold fields [1,2]. For nanostructured carbon materials, i.e. nano-crystalline diamond, carbon nanotube (CNT) and nano-crystal graphite films, emission has been described by tunnelling processes quantified by the Fowler–Nordheim relation:

$$J(F) = A'F^2 e^{\frac{-B'\varphi^{3/2}}{F}}, \tag{1}$$

where F is the applied electric field, φ is the work function and A' and B' are functions defined elsewhere [3]. The FN relation (1) was derived for a metallic emitter at low temperatures and thus does not consider a thermionic component to the emission. While the applied field F for planar geometries is uniform over their surface, nanostructured materials exhibit a strong variation in the local field distribution. The non-uniform field is often described by a field enhancement factor β, which modifies the applied field, F, to $\beta(x, y)\cdot F$. The field enhancement factor has then become a spatially dependent function. Assessing the work function from a current/voltage dataset for a given material involves a fitting procedure using Eq. (1) which requires knowledge about the field enhancement factor β. Thus, a simultaneous computation of φ and β is possible but with limitations.

Temperature dependent or thermionic emission was first formulated by Richardson and is described by the expression

$$J(T) = A_R T^2 e^{-\frac{\varphi}{k_B T}}, \tag{2}$$

where T is the emitter temperature, A_R is the Richardson constant with a theoretical value of 120 A/cm^2 K^2 and k_B is the Boltzmann constant. Under the influence of an electric field this equation becomes modified by introducing a field dependent term in the exponent and is thus given by

$$J(T,F) = A_R T^2 e^{-\frac{\varphi-\sqrt{e^3F}}{k_B T}}, \tag{3}$$

where F is the applied electric field and e the electronic charge. This expression is referred to as the Schottky equation and it accounts for the field dependent barrier lowering.

* Corresponding author. Tel.: +1 919 515 3417; fax: +1 919 513 0670.
E-mail address: fakoeck@ncsu.edu (F.A.M. Koeck).

0925-9635/$ - see front matter © 2006 Elsevier B.V. All rights reserved.
doi:10.1016/j.diamond.2005.12.051

In this study, the field emission characteristics of nano-crystal graphitic films were studied. These films exhibit intense field emission which has been attributed to their nanostructured morphology. The spatial characteristics of the field emission are studied with an electron emission microscope and the current–voltage characteristics are obtained as a function of temperature. The results are discussed in terms of both field emission and field enhanced thermionic emission.

2. Experimental

Nano-crystal graphitic films (nC) were synthesized by chemical vapor deposition utilizing hydrogen as carrier gas and methane as the carbon source [4]. Deposition was commenced at a pressure of 100 Torr under a dc discharge between the substrate and tungsten cathode. The substrate temperature was ~1000 °C with an applied dc voltage of ~800 V between the electrodes resulting in a current density of ~0.25–0.75 A/cm^2. Two samples were studied, one prepared on a silicon wafer and the other on a polished molybdenum disk.

The surface morphology has been evaluated by scanning electron microscopy while emission from the surface was imaged by electron emission microscopy. The latter technique is employed to image in real time surface processes in a controlled UHV environment [5]. Emission from a sample can be imaged at an electric field of up to 10 V/μm and sample temperatures up to 1200 °C.

A different system was employed for thermionic and field emission characterization. The apparatus provides a UHV environment with a base pressure $<5\times10^{-10}$ Torr. For thermionic emission, a radiatively heated sample stage is utilized while a cooled, moveable collector is positioned near the emitting sample. The electric field was determined by applying a measured voltage across the known emitter–collector separation of typically 500–1000 μm. A moveable sample stage with a 25 μm vertical resolution allowed accurate collector positioning. Current/voltage sweeps were recorded at various fields and temperatures using a Stanford Research power unit.

3. Results and discussion

Nano-crystal graphitic films exhibit a surface structure represented by graphitic 'flake-like' crystallites (CNG) as well as carbon nanotubes (CNTs). In a different study the characteristic size of the CNG and CNT elements was determined to be 10–50 nm [6]. From scanning electron microscopy an aspect ratio in the range of 40–600 was determined. This specifies the ratio of the species height and the edge dimension and is directly related to the field enhancement factor β.

The electron emission microscope was employed to image the emission from a nano-crystal graphitic film deposited on Si (Fig. 1). At approximately room temperature, the emission is characterized by intense sites with a strong variation in brightness across the surface. The emission site density as estimated from the acquired image is $\sim3\times10^5$/cm^2. Localized emission can be attributed to a non-uniform spatial distribution of the field enhancement factor β. With the high aspect ratio features present on the surface, the intense field emission sites are attributed to geometric field enhancement of the nanostructures. Here, emission is dominated from regions which exhibit the highest geometric field enhancement. Regions exhibiting a lower field enhancement would correspond to emission sites with reduced brightness. The observed electron emission microscopy image suggests a spatial variation in the geometric field enhancement for the nano-crystal graphitic film. As the emitter temperature is increased a significant reduction in the emission intensity and emission site density (to $\sim1\times10^5$/cm^2) is observed. It was evident that this film could no longer be used to determine the current–voltage characteristics of the emission.

An equivalent nano-graphitic film deposited on a polished molybdenum substrate was used for thermionic and field emission current–voltage characterization. The nanostructured film exhibited a morphology typical for nano-graphitic deposits as shown in the SEM image in Fig. 2. This film is comprised of graphitic flakes and some nanotube like structures are also evident [7].

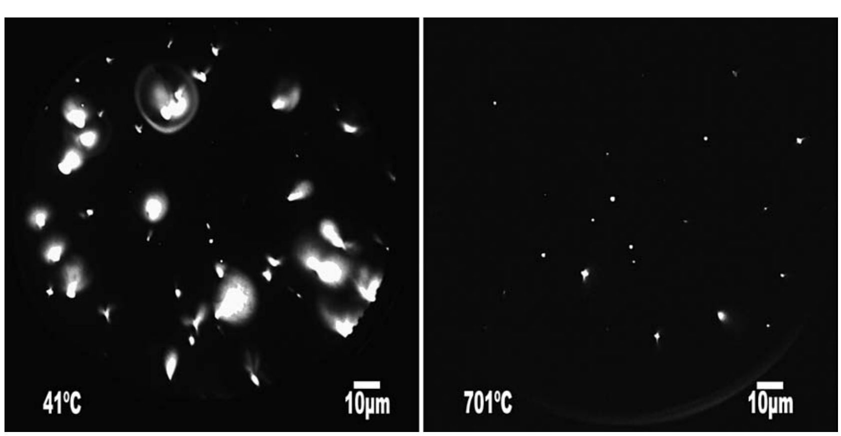

Fig. 1. Electron emission microscopy at two different temperatures from a nano-crystal graphitic film deposited on silicon. A significant reduction in emission site density and emission intensity is observed at elevated temperatures.

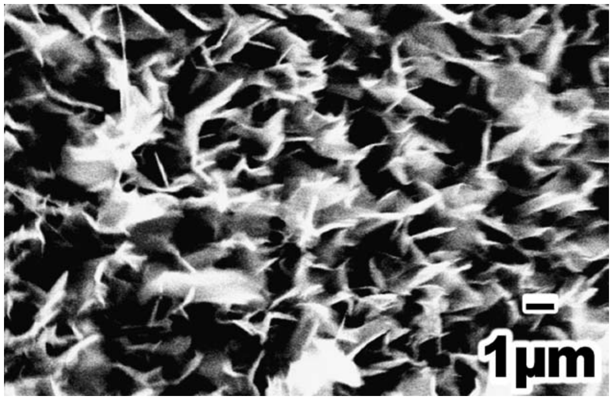

Fig. 2. Scanning electron microscopy image of a nano-crystal graphitic film deposited on a molybdenum substrate.

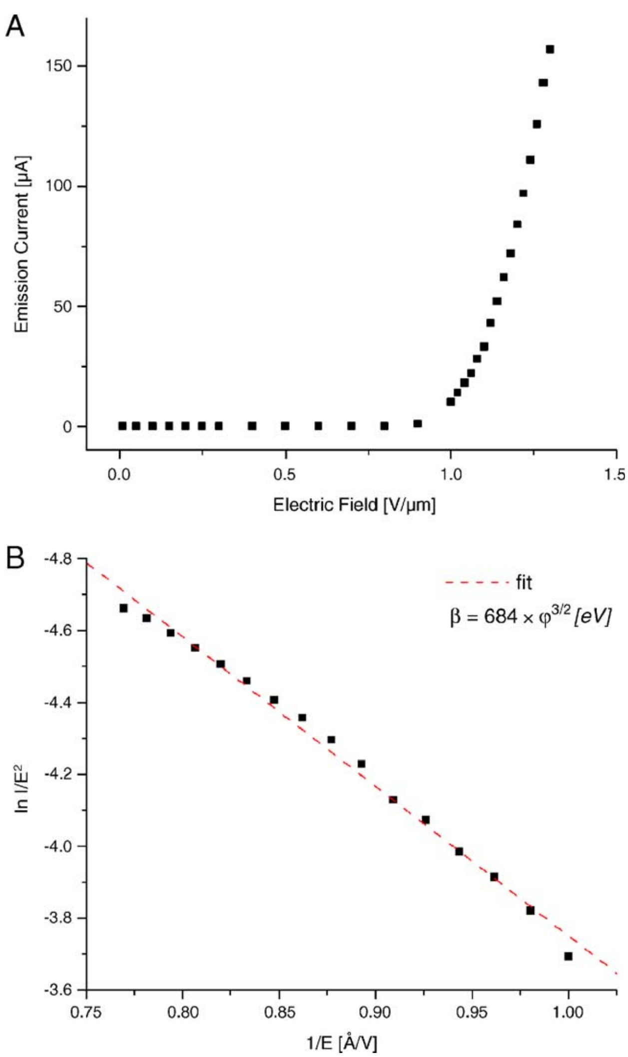

Fig. 3. (A) Current/voltage plot for a nano-crystal graphitic film at room temperature. The film was deposited on a molybdenum substrate and its current increases exponentially with the applied field. (B) Fowler–Nordheim plot of the field emission data in (A). The broken line corresponds to a fit where the slope S has an absolute value of 4.15×10^4 $eV^{3/2}$.

Electron emission shown in Fig. 3 is characterized by an exponential increase of the emission current with applied field. A threshold field of ≤ 1 V/μm is observed and at an electric field of 1.3 V/μm a significant emission current density of ~ 0.77 mA/cm^2 is measured. To further analyze the emission the data is presented in a Fowler–Nordheim plot (Fig. 3B). By fitting the acquired data with the Fowler–Nordheim equation, an estimate for the ratio of work function and field enhancement factor can be obtained. As shown by the fit in Fig. 3B, emission from the nano-crystal graphitic film can be described by a β and φ given by the following relation:

$$\beta = \frac{2.84 \times 10^7}{S} \times \varphi^{3/2}, \tag{4}$$

where S is the slope of the Fowler–Nordheim plot and φ the work function in electron volt. From Fig. 3B an absolute value for S of 4.15×10^4 $eV^{3/2}$ can be extracted.

Determining the field enhancement factor of nanostructured carbon materials is typically based on the assumption of a graphitic work function of ~5 eV. A more distinct experimental evaluation can be achieved by measuring the thermionic emission current and fitting the results to the Richardson–Dushman equation. For multiwall carbon nanotubes this procedure resulted in a work function of ~4.7 eV where similar field emission measurements indicated a work function of 3.9 eV and a field enhancement factor of ~3300 suggesting a shortcoming in the Fowler–Nordheim method when determining the work function [8]. Elsewhere, a work function of ~4.2 eV was determined for a nanosize (5–7 nm) graphite crystal film [9]. For our nano-crystal graphitic films comprised of graphitic 'flake-like' crystallites (CNG) as well as carbon nanotubes (CNTs), a variation in the local work function would result from these two different carbon species. However, the film structure is dominated by flake-like structures suggesting the work function to be uniform for these elements across the film. In this case using a 5 eV work function the Fowler–

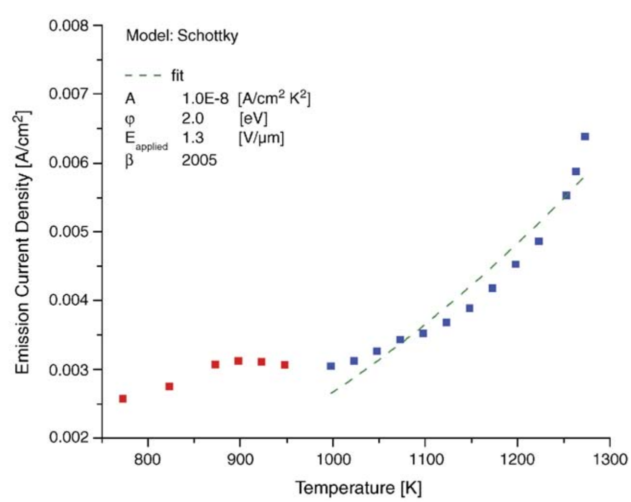

Fig. 4. Current/temperature plot for a nano-crystal graphitic film exposed to an electric field of 1.3 V/μm and a data-fit (broken line) according to a field-modified Richardson equation (Schottky relation).

Nordheim based relation in Eq. (4) would indicate a field enhancement factor β of ~7650. Similarly, a fit with a work function of 2 eV would result in a field enhancement factor β of ~1930. These significant geometric field enhancement factors are higher than values predicted from the experimentally observed surface morphology. Here, a typical structural film element, i.e. the graphitic nano-crystallites, with an edge width of 10 nm and height up to 5 µm would exhibit a geometric field enhancement factor of ~500 [10].

To further explore the emission characteristics, the temperature dependence of the emission was analyzed. The current voltage measurements were repeated as the sample exposed to an electric field is gradually heated and its emission current recorded. Fig. 4 displays a thermionic data plot from a nano-crystal graphitic film where an electric field of 1.3 V/µm is applied between emitter and collector. The emission initially increases as the temperature is increased, then it decreases at ~900 K and increases again above 1000 K.

This initial increase and decrease in the emission behavior may be attributed to the desorption of surface adsorbates from the nano-crystal graphite surface. This emission behavior is observed in the initial temperature dependent current plot. Successive measurements do not exhibit this local minimum in the emission suggesting a desorption process which alters the emission characteristics. For SWCNTs a change in work function depending on the adsorbate species and orientation has been reported as well as an adsorbate induced change in the emission current for MWCNTs [11–13].

Raising the temperature beyond 1000 K yields a strongly enhanced emission current with a current density of ~6 mA/cm^2 at 1000 °C (at an electric field of 1.3 V/µm). This emission behavior is contrary to the electron emission microscope measurements of the sample on a Si substrate where a reduction in emission current was observed. We suggest an interface reaction occurs between the silicon substrate and nano-crystal graphitic film which adversely affects the emission properties.

The increase in emission at 1000 K is suggestive of the field enhanced thermionic emission. We have attempted to reconcile the field enhancement and work function from our thermionic and field emission data. The thermionic data plotted in Fig. 4 can be evaluated with respect to the field-modified Richardson relation, Eq. (3), while room temperature field emission results shown in Fig. 3 can be processed by the Fowler–Nordheim approach. The field term in the field-modified Richardson relation must also include the field enhancement β and using a value for β of 2005 an effective work function of 2.0 eV is calculated. Considering this work function of 2.0 eV and calculating the field enhancement factor after the Fowler–Nordheim related fit in Eq. (4) gives a consistent value for β of 2013.

The field enhancement factor of about 2000 is still larger than the value determined from morphology measurements (~500). This discrepancy may be explained by field penetration effects which are not considered in the Fowler–Nordheim and Schottky emission relations. These effects have recently been proposed to describe the emission from carbon nanotubes. The similarity of CNTs and graphitic nano-crystallites suggests parallels in the emission based on the electronic structure. Here, non-metallic elements are subject to significant field penetration causing a change in the band structure near the emitting surface. These band bending effects will result in a reduced effective work function of the material [14]. It has been shown elsewhere that for a capped CNT with a work function of 4.8 eV, an external electric field of 0.033 V/nm will result in an effective work function of 3.0 eV [15]. In this limited calculation, this external electric field of 0.033 V/nm is only moderately enhanced at the tip of the nanotube by a field enhancement factor of $\beta \approx 3.3$ (due to the small aspect ratio of the CNT). The results indicate that the amount of work function lowering is dependent on the specific structure of the CNT, i.e. open or closed and bonding configuration as well as the termination of the tube end. At the applied field of 0.033 V/nm the work function is decreased by 1.0 to ~1.75 eV depending on the specifics of the structure. Resulting effective barriers of less than 2.0 eV are predicted for some configurations. The calculation suggests that field penetration can play a significant role in the effective barrier for CNT materials. A more detailed study for example, employing the emission model proposed by Stratton, would allow a more distinct investigation of field penetration effects [16].

4. Conclusion

Nano-crystal graphitic films were synthesized on silicon and molybdenum by dc discharge CVD. The samples exhibit a morphology of predominantly graphitic flakes vertically aligned to the substrate surface. Electron emission is localized and attributed to field enhancement effects where geometric features contribute to the field enhancing motive. The temperature dependence of the emission is apparently influenced by surface adsorbates and interface reactions. For nano-crystal graphitic films on molybdenum an increase in the emission is observed as the temperature is increased. The temperature dependent emission is described by a field modified Richardson equation. Through comparison with the geometric field enhancement factor, it is suggested that field penetration may be necessary to account for the observed reduction in the effective work function.

Acknowledgement

This research is supported by the Office of Naval Research through the TEC MURI project.

References

[1] N. de Jonge, Y. Lamy, K. Schoots, T.H. Oosterkamp, Nature 420 (2002) 393.
[2] J.Y. Wang, T. Ito, Diamond and Related Materials 14 (9) (2005) 1469.
[3] A. Modinos, Field, Thermionic and Secondary Electron Emission Spectroscopy, Plenum Press, New York, 1984.
[4] A.A. Zolotukhin, A.N. Obraztsov, A.O. Ustinov, A.P. Volkov, Journal of Experimental and Theoretical Physics 97 (6) (2003) 1154.

[5] H. Ade, W. Yang, S.L. English, J. Hartman, R.F. Davis, R.J. Nemanich, V. N. Litvinenko, I.V. Pinayev, Y. Wu, J.M.J. Madey, Surface Review and Letters 5 (6) (1998) 1257.
[6] A.N. Obraztsov, Al.A. Zakhidov, A.P. Volkov, D.A. Lyashenko, Diamond and Related Materials 12 (3–7) (2003) 446.
[7] A.N. Obraztsov, Al.A. Zakhidov, Diamond and Related Materials 13 (4–8) (2004) 1044.
[8] H.H. Busta, R.J. Espinosa, A.T. Rakhimov, N.V. Suetin, M.A. Timofeyev, P. Bressler, M. Schramme, J.R. Fields, M.E. Kordesch, A. Silzars, Solid-State Electronics 45 (6) (2001) 1039.
[9] A.N. Obraztsov, A.P. Volkov, Al.A. Zakhidov, D.A. Lyashenko, Yu.V. Petrushenko, O.P. Satanovskaya, Applied Surface Science 215 (2003) 214.
[10] S.C. Lim, H.J. Jeong, K.S. Kim, I.B. Lee, D.J. Bae, Y.H. Lee, Carbon 43 (13) (2005) 2801.
[11] C.W. Chen, M.H. Lee, Diamond and Related Materials 12 (3–7) (2003) 565.
[12] A. Maiti, J. Andzelm, N. Tanpipat, P. von Allmen, Physical Review Letters 87 (15) (2001) 155502.
[13] K.S. Yeong, J.T.L. Thong, Applied Surface Science 233 (1–4) (2004) 20.
[14] C.W. Chen, M.H. Lee, S.J. Clark, Applied Surface Science 228 (1–4) (2004) 143.
[15] X. Zheng, G.H. Chen, Z. Li, S. Deng, N. Xu, Physical Review Letters 92 (10) (2004) 106803.
[16] R. Stratton, Physical Review 125 (1) (1962) 67.